MECHANICAL CHARACTERISTICS AND CHEMICAL PROPERTIES OF ASTM A516 GRADE 70 CARBON STEEL

H. Muhamad Hellmy[1*] ,C.L. Nur Azida[1] and M.Z. Norazwani[1]

[1]Joining and Fabrication Engineering Technology,
Universiti Kuala Lumpur Malaysia France Institute (UniKL MFI), 43650 Bandar Baru Bangi, Selangor Darul Ehsan, Malaysia.

*Corresponding Author's Email: hellmy@unikl.edu.my

Article History: Received 3 February 2026; Revised 19 June 2026; Accepted 8 July 2026

ABSTRACT: Carbon steel, mainly composed of iron (Fe) and carbon (C), accounts for approximately 90% of global steel production. ASTM International (ASTM) A516 Grade 70 is a common type used in pressure vessels, boilers, and processing equipment where improved notch toughness is required. It also offers a good balance of strength and weldability, making it ideal for low- to moderate-temperature applications. Despite its widespread use in the oil and gas industry, limited data have resulted in limited understanding of its properties. Thus, this study examines the mechanical and chemical properties of ASTM A516 Grade 70, a low- to medium-carbon alloy steel. Specimens were tested for tensile strength (ASTM E8), bend resistance (ASTM E290), and hardness (ASTM E92-17). Notably, polishing was applied when necessary. Furthermore, microstructure was analyzed using a Field Emission Scanning Electron Microscope equipped with Energy Dispersive Spectroscopy (FESEM-EDS), while X-ray Diffraction (XRD) examined phase composition. In addition, FESEM-EDS confirmed the presence of Fe and C elements, whereas XRD revealed clear C peaks at 2θ values of 29.46°, 35.21°, 46.86°, 47.79°, and 60.09°. Overall, these findings are consistent with the chemical composition, with C content ranging from 0.17% to 0.28%, and are further supported by line-scan mapping. Concurrently, hardness values strongly correlated with mechanical behavior, confirming the material's suitability for structural and high-pressure applications.

KEYWORDS: *A516 Grade 70; microstructure; mechanical strength; FESEM-EDS; XRD*

1.0 INTRODUCTION

ASTM International (ASTM) A516 Grade 70 is classified as a ferrous metal within the carbon steel alloy group, which is primarily composed of iron (Fe) and carbon (C). Generally, carbon steel is often alloyed with various elements to achieve specific desired properties. The term carbon steel refers to steel containing a C content of 0.05% to 2.1% by weight (Prieto et al., 2018). The C weight percentage indicates that as the C content increases, steel can become harder and stronger. It further specifies the percentage content of other elements, which can add value by improving the strength and toughness of carbon steel. Beyond these, heat treatment can increase the steel's mechanical strength. Nevertheless, heat treatment also introduces disadvantages, such as reduced weldability and decreased steel ductility [1]. Carbon steel is widely used in industry and is classified into four categories based on C content: Low-Carbon (L-CS), Medium-Carbon (M-CS), High-Carbon (H-CS), and Ultra-High Carbon Steel (UH-CS). L-CS, commonly referred to as mild steel, contains approximately 0.05 to 0.3% C content. Meanwhile, M-CS has approximately 0.3 to 0.6%; H-CS has approximately 0.6 to 1.0%; and UH-CS has approximately 1.25 to 2.0%. In addition to Fe and C, other major elements include manganese (Mn), silicon (Si), tungsten (W), and chromium (Cr) [2].

ASTM A516 Grade 70, also referred to as American Society of Mechanical Engineers (ASME) SA516 Grade 70, is a widely utilized carbon steel in the industry. This is particularly true for boiler and pressure vessel applications. Most pressure vessels and boilers are designed to contain gases or liquids under specific pressure and temperature conditions. Therefore, in some applications, metal pressure vessels require adequate mechanical strength, which is provided by carbon steels [3]. In terms of chemical composition, this metal contains various alloying elements in its chemical composition. This includes sulfur (S), Mn, Si, and phosphorus (P), permitted by the ASTM grade. These elements aim to produce the hardest and strongest steel plates in accordance with the ASTM specification. Compared with other steel grades, it has high yield and tensile strength and has the ability to absorb impact when a flaw is present. Furthermore, this material exhibits good resistance to lamellar tearing, sulfur (S) corrosion, and hydrogen (H)-induced damage, while also having a low deformation temperature [4]. In A516 Grade 70, C plays a key role in enhancing wear resistance and hardenability during heat treatment.

Research has reported that a C content of 0.1 wt% provides optimal toughness in chromium-molybdenum (Cr-Mo) pressure vessel steel. Despite this, when C exceeds 0.2 wt% in carbon steel, it forms hard microstructures such as martensite or bainite, which are prone to H-induced cracking.

Following this, Si is mainly added to carbon steel as a deoxidizer to improve strength and hardenability. It also enhances oxidation resistance and helps prevent carburizing at high temperatures. Still, excessive amounts of Si should be avoided, as it can negatively impact toughness and weldability [5]. For example, the combination of 0.5% Mo and 0.08% oxygen (O) forms a coarse ferrite (α-Fe) grain boundary. Additionally, high Mo content is harmful when low-temperature toughness is desirable. Conversely, a high Si content (0.8%) could negatively affect the material's toughness. Moreover, Mn improves the tensile strength of A516 Grade 70 without reducing ductility, since C contributes to the metal's hardenability. In essence, Mn helps reduce distortion when heat is applied to the metal [6].

This research examines the mechanical and chemical properties of A516 Grade 70 carbon steel to advance knowledge. Specifically, the study aims to provide detailed insights into the tensile strength, bending properties, hardness, and microstructure of A516 Grade 70 carbon steel. These findings will help engineers make informed material choices during the design phase, particularly for costly materials, and provide valuable information on steel commonly used in industrial applications.

2.0 MATERIALS AND METHODS

2.1 Sample Preparation and Mechanical Testing

In this study, 6 mm-thick ASTM A516 Grade 70 carbon steel plates were used as test samples. Following the cutting process, tensile, bend, and hardness tests were conducted. The mechanical testing followed ASTM E8 Standard Test Methods for Tension Testing of Metallic Materials. Following this, dog-bone samples measuring 250 mm x 50 mm x 6 mm were prepared for the tests. Correspondingly, the tensile test provides valuable data on a material's strength and ductility under uniaxial tensile stress. Thus, the test is important for comparing the metal's strength. The tensile test was performed on an Instron 5980 Series Universal Testing Machine with a 250 kN force capacity, equipped with

Bluehill software.

Another crucial mechanical test in this study is the bend test. Test coupons measuring 200 mm x 40 mm x 6 mm were then prepared in accordance with ASTM E290, the Standard for Bend Testing. This test provides important data to assess the metal's ductility. Additionally, the hardness test was conducted in accordance with ASTM E92-17 Standard Test Methods for Vickers Hardness of Metallic Materials. A force of 10 kgf was applied, with a dwell time of 10 seconds at each testing point.

2.2 Metallography Examination and Phase Analysis

Samples of the required dimensions were extracted from ASTM A516 Grade 70 carbon steel plates. Cross-sectional specimens were prepared by cutting the material into 10 mm (length) × 10 mm (width) × 10 mm (thickness) specimens using a wire cutter following the appropriate sample preparation procedure. The specimens were subsequently subjected to microstructural and elemental analysis using a Field Emission Scanning Electron Microscope equipped with Energy Dispersive Spectroscopy (FESEM-EDS). FESEM-EDS was used to obtain high-resolution images and to examine the elemental distribution of the specimens. An accelerating voltage of 10 kV was applied throughout the analysis, with an estimated penetration depth of approximately 1.5 µm.

Prior to FESEM-EDS analysis, the specimens were cleaned with ethanol to remove surface contaminants and lose residues and were subsequently mounted in resin to facilitate handling during analysis. No additional grinding or polishing was performed because the FESEM-EDS analysis was intended to examine the prepared specimen surface. The specimens were carefully handled after cleaning to minimize contamination and disturbance of the surface. Since the specimens were analyzed without additional polishing, possible effects of surface roughness and topographical variations on the FESEM images and EDS line-scan results were considered during interpretation.

The process of preparing and cutting the samples for phase characterization by X-ray Diffraction (XRD) is the same as that for surface morphology characterization by FESEM-EDS. The sample was cut to 10 mm (length) x 10 mm (width) x 5 mm (thickness) using a Diamond Cutter Machine. After cutting, the sample was polished using the Metaserv model 2000 to flatten its surface. Therefore, the X-rays can be directly aimed at the smooth, flat surface. Phase characterization is performed by XRD on a Rigaku Miniflex II. X-rays are a type of electromagnetic radiation with photon energies ranging from 100 eV to 100 keV. Their ability to penetrate various materials makes them essential for applications in medical imaging and materials analysis. Thus, Parameter 2 (ranging from 3 to 80) was used in XRD applications. Concurrently, X-ray shortwave radiation in the range of 1 keV to 120 keV was used due to its ability to penetrate the atomic and molecular structures of this type of metal.

3.0 RESULTS AND DISCUSSION

3.1 Characteristics of A516 Grade 70 Raw Metal

Characterization analysis was conducted on A516 Grade 70 carbon steel raw metal, as illustrated in Figure 1. The primary raw material used in this research was ASTM A516 Grade 70, commonly referred to as ASME SA516, selected as the main metal plate for experimentation and analysis. This material was sourced from CW Hardware Sdn. Bhd. The metal plate is widely utilized in construction for its high strength and durability. In particular, it is commonly employed in the industry for manufacturing pressure vessels and boilers for its toughness. Additionally, its weldability and enhanced notch toughness make it an ideal candidate for these applications. Table 1 presents the chemical composition of the raw material, while Table 2 outlines the standard mechanical properties of A516 Grade 70 carbon steel.

Table 1: Chemical composition in (wt%) of base metal and welding electrode

	C	Mn	P	S	Si	Al	Cu	Ni	Cr	Mo	Ti	V
A516 gr. 70	0.28	1.14	0.019	0.008	0.24	0.054	0.02	0.01	0.02	0.002	0.004	-
E-7018	0.07	0.87	0.015	0.011	0.61	-	-	0.02	0.03	0.01	-	0.01

Table 2: Mechanical properties of ASTM A516 Grade 70 carbon steel

Mechanical properties	Metric value
Tensile strength	485 - 620 MPa
Yield strength	260 Mpa
Elongation at break (in 200 mm)	17%
Elongation at break (in 500 mm)	21%
Modulus of elasticity	200 GPa
Poisson's ratio	0.29
Shear modulus	80 GPa

Figure 1: Raw metal plate ASTM A516 Grade 70 carbon steel plate

3.2 Microstructure and Hardness of Raw A516 Grade 70 Carbon Steel

Figure 2 depicts the surface microstructure image of A516 Grade 70 carbon steel raw metal sample prior to being subjected to any mechanical testing. As displayed in Figure 2, the raw metal sample consists of α-Fe (white) and pearlite (black) phases. Accordingly, α-Fe is a microstructural phase characterized by its softness and ductility, resembling the properties of pure Fe. Meanwhile, pearlite is a combination of α-Fe and cementite (Fe_3C), with Fe_3C exhibiting ceramic-like properties that make it very hard and brittle. Following this, the pearlite phase consists of alternating layers of α-Fe and Fe_3C. In comparison, the α-Fe phase exhibited a brighter color compared to the pearlite phase due to the softer characteristics of the α-Fe relative to those of pearlite [7].

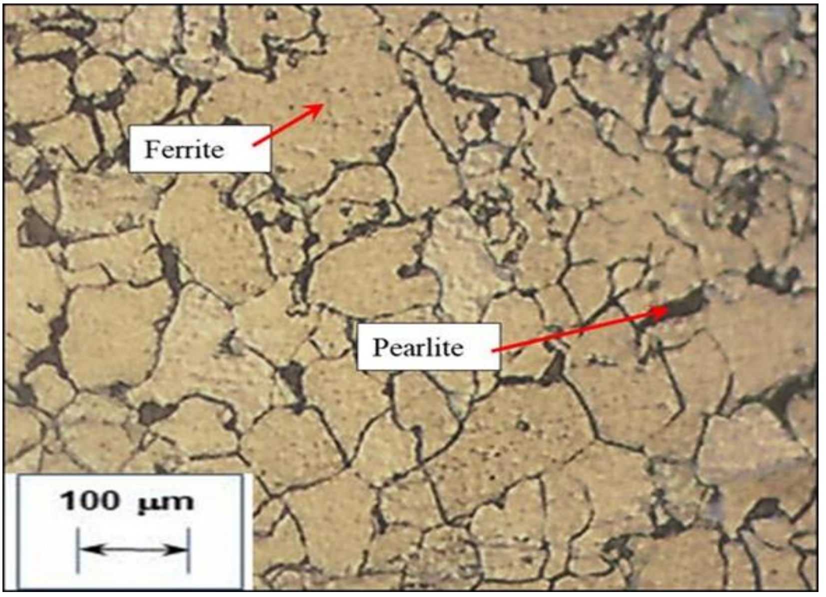

Figure 2: Surface microstructure image of A516 Grade 70 carbon steel using an optical microscope

The microstructure illustrated in Figure 2 is consistent with the claim that the A516 Grade 70 raw metal has a high C content, ranging from 0.17% to 0.28%. This C-Mn steel type is classified as a medium-high-carbon steel grade for moderate and low-temperature applications in accordance with Pressure Vessel Quality (PVQ) standards [8]. Remarkably, this carbon steel type presents excellent resistance to sulfuric acid and chlorides in harsh environments. In addition, Prieto et al. [9] noted that almost all construction boilers and pressure vessels, including their components, are made of carbon steel, which is widely used in the oil, gas, and petrochemical industries. Building on this, it is typically categorized into several groups: (i) low carbon steel (0.15% max. C), (ii) medium-low carbon steel (0.15-0.23% C), (iii) medium-high carbon steel (0.23-0.44% C), and (iv) high carbon steel (more than 0.44% C) [9].

The micrograph image of A516 Grade 70 depicted in Figure 2 was confirmed by Ibrahim et al. [10]. The study presented the typical α-Fe-pearlite microstructure characteristic of similar carbon steel grades used to manufacture pressure vessels, boilers, and storage tanks across various industrial sectors for low and moderate working temperatures [10-11]. Moreover, Oyyaravelu et al. [11] confirmed that the A516 Grade 70 carbon steel was predominantly composed of an α-Fe-pearlite structure with some fine, dispersed alloy carbide particles. Bakhtiari and Zangeneh [12] further agreed that the base metal of A516 Grade 70 carbon steel had an α-Fe-pearlite structure with MnS particles [13]. The typical microstructure of A516 Grade 70 carbon steel, reported by Prajapati and Badheka [13], closely agreed with that reported in the current investigation. They established that the microstructure consisted of large α-Fe grains with some colonies of pearlite [12-15]. There were also some degenerate pearlites. Accordingly, α-Fe is characterized by its softness and ductility, whereas pearlite is known for its hardness and brittleness. According to Figure 2, the C content of ASTM A516 Grade 70 is 0.17% to 0.28%, indicating that the pearlite content is higher and tends to increase the bulk strength. In addition, the fine α-Fe microstructure can be a key factor influencing the hardness of carbon steel [16]. On the other hand, the phase and chemical composition details agreed with the EDS line-scanning mapping and the XRD patterns illustrated in Figures 6 and 7.

Figure 3 depicts the hardness value of A516 Grade 70 carbon steel raw metal. The sample yields hardness values of 165–190 HV. This is due to the high C content in A516 Grade 70 carbon steel. Rather than C content, Si contributed to the hardness of the carbon steel, as described by Otani and Sasaki [17]. They reported that the Vickers microhardness increased proportionally with increasing Si content. As hardness increased, tensile strength and elongation at break also increased [17]. In this case, the measured hardness value in Figure 3 was compared with that reported by Corigliano et al. [18] for a similar carbon steel type. They reported a hardness value of 175 HV, which falls within the range of the measured current value, with slight inconsistencies in the data analysis [18]. Overall, it falls within the common range for carbon steel, as the steel has a high C content and other alloying elements, such as Si and Mn, with high hardenability [19].

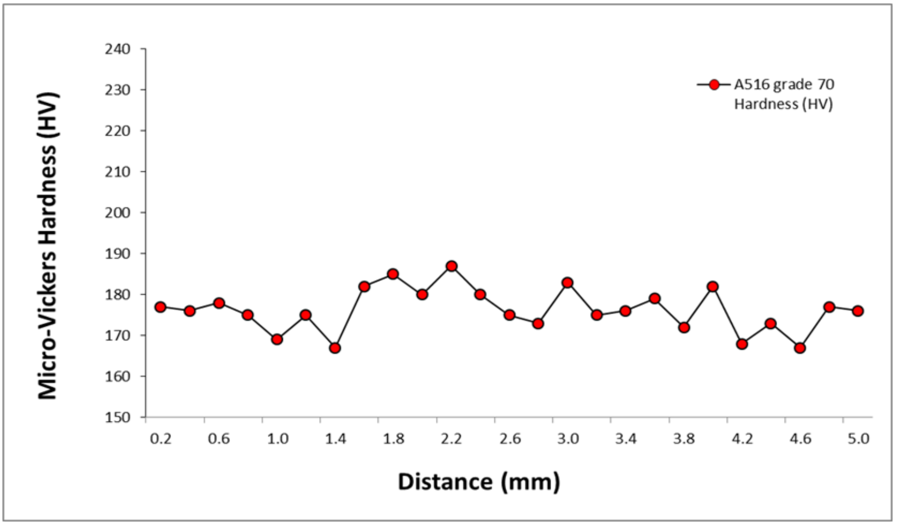

Figure 3: Hardness result of A516 Grade 70 carbon steel raw metal

Hardness characteristics are directly related to mechanical properties. Based on the hardness characteristics and the results presented in Figures 2–5, A516 Grade 70 carbon steel demonstrated exceptional mechanical performance under stress, combined with advantageous low-cost features. This makes it the primary choice for commercial plants and the oil and gas industry [20]. This type of carbon steel has good yield strength, but its performance decreases as temperature increases. In addition to C content, hardness characteristics are also well correlated with other chemical composition percentages, such as Mn and Si [21]. In this regard, the following section discusses the benefits of its mechanical properties and the role of its chemical composition in determining its overall performance in various applications.

3.3 Mechanical Characteristics of Tensile and Bend Tests

Most materials, especially steel, are typically subjected to stresses or loads during operation. Therefore, understanding the material's stress-strain behavior is essential, as impacts or collisions can cause deformation during operation. The most frequently conducted mechanical tests involve tension and bending [22]. A tensile test, also known as a tension test, is a destructive testing method in engineering that applies controlled stress to a sample until it ultimately fails, allowing for evidence-based analysis. A uniaxial tensile load is applied along the sample's long axis, and the sample's shape changes during testing. In this work, tensile and bend tests were performed to evaluate the mechanical properties of A516 Grade 70 raw carbon steel. Specifically, the objective is to examine the mechanical properties of A516 Grade 70 raw carbon steel before it breaks and how much it can extend. This test method assesses yield strength, ultimate tensile strength, and ductility. The engineering stress (σ) is defined by equation (1):

$$\sigma = \frac{F}{A^o}, \tag{1}$$

where F is the instantaneous load applied perpendicular to the sample's cross-section, and Ao is the original cross-sectional area before any load is applied. The engineering strain (ε) is defined in equation (2):

$$\varepsilon = \frac{l_i - l_o}{l_o} = \frac{\Delta l}{l_o}, \tag{2}$$

where l_o is the original length before any load is applied, and Δl is the deformation, elongation, or change in length at some instant, as referenced to the original length.

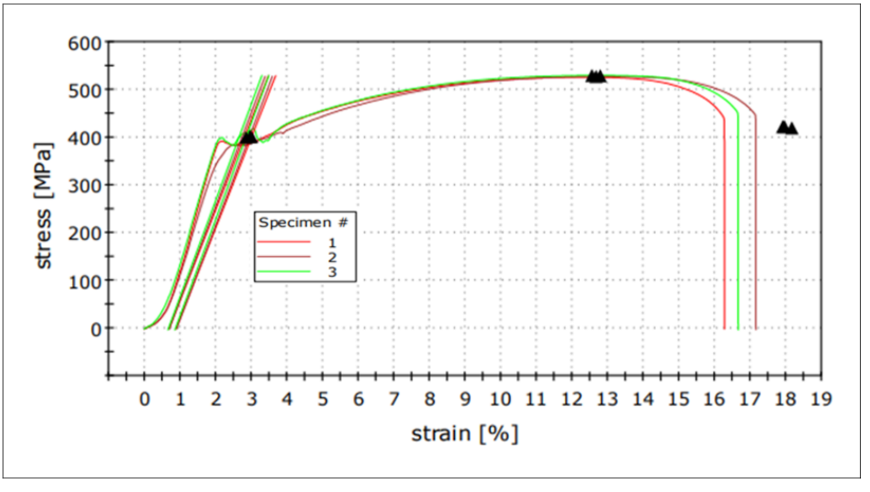

Figure 4: Tensile test result of A516 Grade 70 carbon steel parent metal

Three test samples (Figure 4) were prepared and tested in accordance with ASTM E8, Standard Test Methods for Tension Testing of Metallic Materials. The specimens were prepared according to the required dimensions specified in the standard. The tensile properties of the flat

ASTM A516 Grade 70 carbon steel specimens were evaluated through tensile testing. The engineering stress and strain were determined from the recorded load and extension data using Equations (1) and (2), respectively.

Figure 4 and Table 3 present the mechanical properties obtained from the tensile tests of ASTM A516 Grade 70 carbon steel. All three specimens exhibited similar load-extension behaviour within the proportional region. The specimens achieved an average ultimate tensile strength of 527.41 MPa and an average yield stress of 386.77 MPa. At the end of the tensile test, fracture occurred approximately at the middle of the gauge length of the specimens. The average tensile stress at fracture was 442.37 MPa, while the average elongation at break was 0.166 mm/mm.

The apparent modulus obtained from the load-extension response ranged from 24.16 to 26.95 GPa, with an average value of 25.60 GPa. This value is considerably lower than the typical Young's modulus of carbon steel, which is approximately 200 GPa. Therefore, the reported value is considered an apparent modulus associated with the measured load-extension response rather than the intrinsic Young's modulus of the ASTM A516 Grade 70 carbon steel. The difference may be attributed to the method used to obtain the extension data and the contribution of deformation and compliance from the testing system, which can have a significant influence on the calculated slope in the small-strain elastic region. Consequently, the value of 25.60 GPa should not be interpreted as the intrinsic elastic modulus of the material. Nevertheless, the measured yield stress and ultimate tensile strength demonstrate the expected tensile behaviour of ASTM A516 Grade 70 carbon steel.

Table 3: Mechanical properties of ASTM A516 Grade 70 carbon steel

Sample	Ultimate Tensile Strength (MPa)	Apparent Modulus from Load-Extension Response (GPa)	Yield stress (MPs)	Elongation at Break (mm/mm)	Tensile stress at break (MPa)
1	525.77	26.95	391.59	0.163	435.39
2	527.22	24.16	371.72	0.171	444.01
3	529.42	25.70	397.01	0.166	447.71
average	**527.41**	**25.60**	**386.77**	**0.166**	**442.37**

Additionally, Figure 5 and Table 4 present the results of the bend tests conducted on ASTM A516 Grade 70 carbon steel. The bend tests were performed in accordance with ASTM E290, Standard Test Methods for Bend Testing of Material for Ductility. Four specimens with similar dimensions were subjected to gradually increasing bending loads until the specified bending condition or failure was reached. The maximum applied load and corresponding deformation were recorded for subsequent analysis. The test provided an indication of the material's resistance to bending deformation and its ability to withstand the applied bending load.

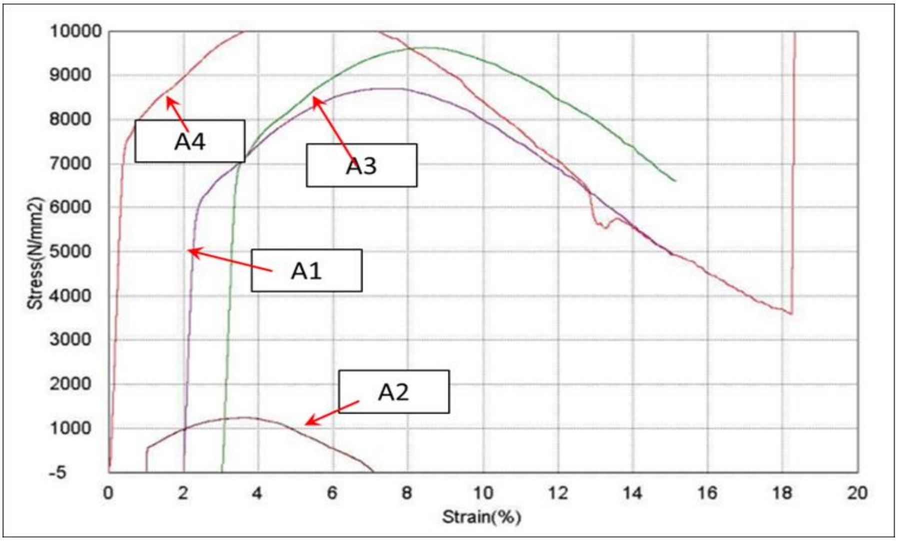

Figure 5: Bend test result of A516 Grade 70 carbon steel parent metal

The four (4) test specimens with similar dimensions were tested by gradually increasing the bending load until the specified test condition or failure was reached, and the corresponding load was recorded for analysis. As presented in Table 4, the bend test results provide an indication of the resistance of ASTM A516 Grade 70 carbon steel to bending deformation. Although the specimens were prepared with similar dimensions and tested under similar conditions, differences in their responses to the applied bending load were observed.

In particular, specimen A2 exhibited a substantially lower maximum flexural stress of 123.98 MPa and a maximum flexural strain of 2.57% compared with the other specimens. This variation may be attributed to minor differences in specimen preparation, surface condition, specimen positioning, or alignment during the bending test. As the specific physical cause could not be conclusively determined from the available experimental observations, the A2 result was retained as an outlier rather than excluded from the analysis. The maximum flexural stress values were re-examined following the reviewer's observation, particularly with respect to the calculation of scaling and unit conversion. The revised maximum flexural stress values ranged from 123.98 to 1,106.56 MPa, with an average value of 767.72 MPa. The average flexural strain was 7.98%. The corrected results are presented in Table 4.

Table 4: Mechanical properties of ASTM A516 Grade 70 carbon steel

Sample	Maximum flexural stress (MPa)	Maximum flexural strain (%)
A1	870.15	18.53
A2	123.98	2.57
A3	970.18	5.37
A4	1106.56	5.45
Average	767.72	7.98

3.4 FESEM-EDS and X-ray Diffraction (XRD)

Figures 6 and 7 illustrate FESEM-EDS and XRD results of the raw material of A516 Grade 70 carbon steel. The FESEM-EDS (Figure 6) results exhibit the line-scanned map of chemical element distribution from the emission spectra of the scanned carbon steel surface plate. The line-scanned map mainly varied with the dominant C and Fe lines, with trace O peaks. Moreover, the results indicated that the A516 Grade 70 carbon steel sample has a high Fe concentration. The trace C peaks suggest that it is the second-highest concentration peak after O.

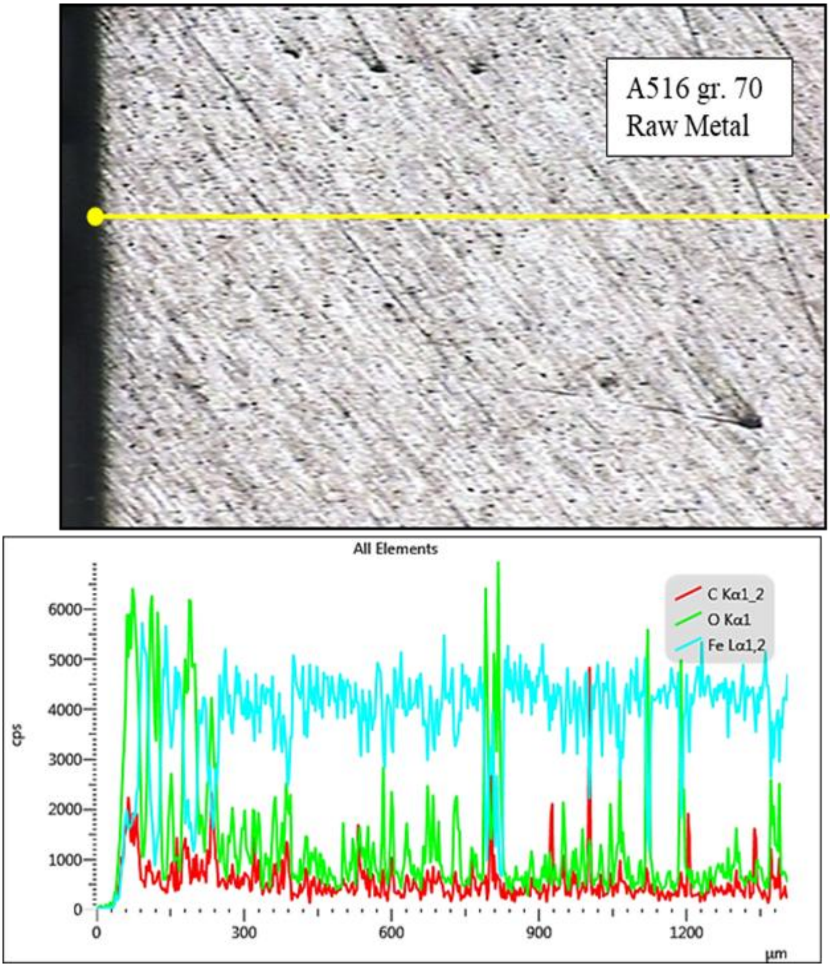

Figure 6: FESEM-EDS line-scanned map of A516 Grade 70 carbon steel raw metal

As verified through XRD analysis in Figure 7, the peaks at 2θ values of 20.66°, 23.07°, 38.68°, 42.43°, 46.86°, and 47.79° represented the traces of C peaks. The peaks at 20.66° and 23.07° could be attributed to a low-angle reflection from a carbide structure or an impurity phase. Meanwhile, the peaks at 38.68°, 42.43°, and 46.86° may be related to Fe_3C's diffraction pattern. The presence of C in A516 Grade 70 carbon steel raw metal strongly agrees with the sample's chemical composition, which has a high C content of 0.17% to 0.28%. This is confirmed by the line-scanned map in Figure 6 and supported by the presence of pearlite, as confirmed by the hardness values in Figures 2 and 3 [23]. Notably, the strongest peak was indicated by the presence of Fe at 2θ values of 44.96° (110) and 65.08° (200). The major peaks correspond to the specific planes in the Body-Centered Cubic (BCC) structure of α-Fe, in which the primary crystalline phases of Fe are established in carbon steel. Specifically, the (110) plane is the most intense and prominent peak, indicating a high degree of crystallinity in the steel. In contrast, the (200) plane corresponds to another significant peak, which highlights the presence of α-Fe in the steel. The others recorded at 29.46°, 49.76°, and 60.09° were evenly distributed, as confirmed by MnO_2 in Figure 7. The common crystalline phase of MnO was discovered in carbon steel A516 Grade 70 since Mn is one of the elemental compositions that ranges from 0.85 – 1.2%. Mn increases the hardenability and tensile strength of carbon steel, but to a lesser extent than C. The presence of MnO_2 implies its inclusion in the steel, influencing its microstructure and mechanical properties. It can also act as a nucleation site for the formation of certain phases during heat treatment. A slight trace of silicon dioxide (SiO_2) at 35.21° was detected in the raw A516 Grade 70 metal, which was unexpected and can be considered a minor signal given the single-peak detection. The peak could correspond to a particular crystallographic plane in the quartz structure. Otherwise, the presence of SiO_2 in the raw A516 Grade 70 metal could be due to contamination during processing, as it suggests a low-intensity peak signal. The heights of peaks, in general, are not proportional to the concentration of elements since they vary with differences in adsorption. Nevertheless, higher intensity can indicate element enrichment, with or without superimposed peaks.

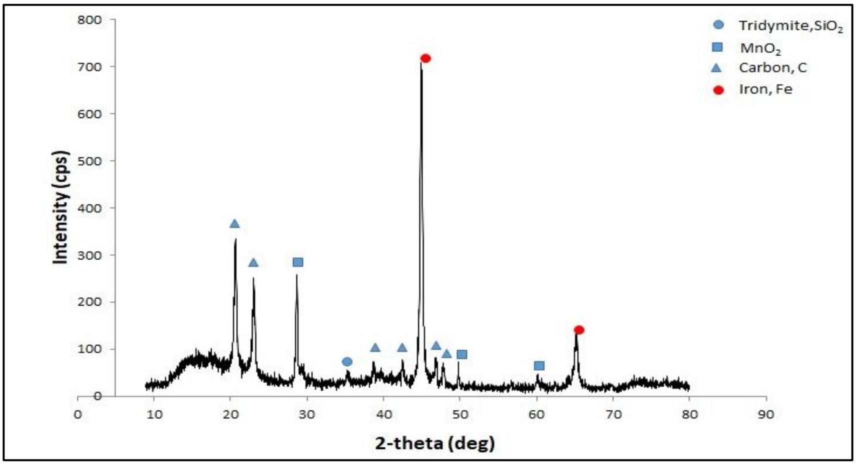

Figure 7: XRD pattern of A516 Grade 70 carbon steel raw metal sample

As illustrated in Figures 6 and 7, A516 Grade 70 carbon steel is a ferrous metal, as confirmed by the presence of major Fe peaks. It primarily consists of Fe, with small amounts of C, Mn, Si, and other elements. The

Fe in this steel is predominantly in the BCC phase at room temperature. XRD confirmed that the majority of the material is composed of Fe in the α-Fe phase. This is further supported by studies by Ali Khan et al. [24], Ibrahim et al. [10], and Sivakumar et al. [25], which reported that the base metal in A516 Grade 70 is Fe. In general, carbon steel, which is composed of nearly 98-99% Fe, is the most widely used and cheapest metal in the fabrication industry. The peaks of Fe, together with other alloying elements such as C and Si, in A516 Grade 70 carbon steel presented superior mechanical properties, including high strength, as demonstrated by the hardness readings in Figure 3 [10, 24-25].

The presence of C peaks in A516 Grade 70 carbon steel indicated a second major alloying element that enhanced the steel's mechanical properties, as depicted in Figure 7. According to the 2θ values in Figure 7, the peaks of C may indicate C-containing phases or compounds. It does not demonstrate strong, distinct XRD peaks due to its low X-ray scattering factor. Although the scattering peak is low, it can be suggested that the presence of C would most likely be initiated through the formation of carbides, such as Fe_3C. The peaks of C were confirmed by Da Luz et al. [26], who reported that high C content was common for this type of steel, as it exhibited high hardenability, high hardness, and high brittleness with low ductility. In line with this, steel becomes harder and stronger as the C content increases. Yu et al. [27] reported that C content played an important role in bonding strength at temperatures below 850°C. By adding C, this element acts as a key austenite stabilizer. As the C content increases, a fully austenitic microstructure can be achieved. Thus, it could have positive effects and reduce residual stresses in the metal [26-27]. It was reported that adding C to the Cr-N coatings reduced their friction coefficient. It also enhanced the mechanical and wear properties of the coatings. In conclusion, the composite C coating was determined to relieve the residual thermal stresses during cooling from the hot-pressing temperature. As emphasized by Saewe et al. [28], it is important to keep C content within its limits. This was further agreed upon by Feng et al. [29]. They assumed that a low C content can avoid high-C martensite and reduce its brittleness. Instead, using this type of carbon steel resulted in significantly lower costs and greater economic benefits [28-29].

Furthermore, a common disadvantage of high C content is that the steel becomes less ductile, making it difficult to weld, machine, or forge [30]. Similarly, Alias et al. [30] noted that C is vital for hardening the steel surface, which resists wear and tear, even though it reduces some important mechanical properties. Instead of C's benefits, Sun et al. [31] identified several drawbacks of adding C to steel. They indicated that morphology and carbide precipitation significantly affected mechanical properties. They found that exceeding the limit can cause complex changes, such as increased impact toughness. However, the steel's strength may decrease continuously, especially when involving heat [31]. Excessive C from carbides may increase local stress concentrations, which may initiate cracks. These carbide formations possess high hardness and brittleness, which might become sites of weakness. Eventually, this can cause failure under stress. Although mechanical properties decreased with increasing C content, this type of metal can be easily enhanced compared with alloyed steel. Saewe et al. [28] agreed with Sun et al. [31] that, due to C content, excessive carbide formation may affect the toughness of the steel. They assumed that larger carbide amounts lead to more incoherent precipitates. When carbides precipitate incoherently, the carbide phase does not match or align well with the host matrix, resulting in a weaker interface bond. As such, this misalignment could serve as a site for stress concentration.

As illustrated in Figure 7, in addition to C, a trace of SiO_2 was also detected on A516 Grade 70 carbon steel. The presence of minor, low-intensity SiO_2 peaks could be attributed to contamination during various stages, such as handling of steel, during which particles can be deposited on the steel surface. It can also be introduced during cutting, grinding, or polishing processes, which often involve abrasive materials that contain silica. Accordingly, SiO_2 is likely to form on the surface of A516 Grade 70, since the steel is a Si-containing material in the vicinity. This can happen through the oxidation of Si present in the steel itself, although in low quantities. In this regard, the presence of SiO_2 on the raw A516 Grade 70 metal is likely due to surface contamination. Following this, the low peak intensity suggests minimal yet detectable contamination. The trace of Si was confirmed by Ali Khan et al. [24] and Zaroog et al. [32], who reported that the Si added in A516 Grade 70 presented the most common alloying element in carbon steel that acts as a deoxidizer and impurity remover [24, 32]. This aligns with our observations of low-intensity SiO_2 peaks in the XRD analysis of A516 Grade 70 steel, suggesting a similar contamination mechanism in our sample. It is well established and consistent with previous findings reported by Zarei et al. [33], which demonstrated specific roles for Si as a deoxidizer, mainly affecting the corrosion resistance of carbon steel. In general, Si promoted heterogeneous distribution and segregation in the Fe matrix. This heterogeneous condition makes high-temperature deformation in Si-containing steels quite different from that in other elements [33]. In contrast, Prajapati et al. [13] reported reduced Si and Mn, possibly due to reaction with O during oxidation.

The presence of MnO_2 in A516 Grade 70 steel, as indicated by diffraction peaks at 29.46°, 49.76°, and 60.09°, suggests that Mn within the steel has oxidized to form MnO_2. Several factors can explain this even distribution of MnO_2 throughout the material. As the role of Si, Mn is commonly added to steel to improve strength, toughness, and wear resistance. Despite this, during manufacturing, Mn can react and be exposed to an O-rich atmosphere. This may form a stable oxidation product, leading to MnO_2. Instead, MnO_2 is a thermodynamically stable oxide that, once formed, tends to remain within the steel structure. Another factor is potential impurities in MnO_2, which could influence the steel. Similar studies related to the influence of other elements on the formation of MnS have been reported in the literature [12]. The MnS content is another factor that contributes to the high corrosion rate of this steel. It focuses on Si addition, which decreases the S and Mn contents and could also reduce the corrosion rate of A516 steel, leading to metal degradation. Hence, the disadvantage of impurities such as MnO_2 is clearly explained: these impurities need to be kept in limited amounts. The presence of MnO_2 in A516 Grade 70 can damage the steel, affecting its mechanical properties, corrosion resistance, and overall performance. Essentially, MnO_2 is a brittle oxide, and its presence in the steel matrix can lead to embrittlement by creating stress concentration sites. It may reduce ductility, making it less capable of deforming plastically before fracturing [34].

Overall, the detection of SiO_2 and MnO_2 in A516 Grade 70 steel, as evidenced by specific diffraction peaks, provides insight into oxidation processes during manufacturing. Consequently, understanding these oxidation products is crucial for predicting the material's long-term performance and tailoring processing techniques to minimize their formation. Moreover, MnO and MnO_2 can influence the steel's corrosion resistance and mechanical properties. While MnO may contribute to the formation of a protective oxide layer, the presence of MnO_2, particularly if unevenly dispersed, could lead to localized stress concentrations, potentially affecting the material's toughness [35]. Regarding the roles of C and Si, with their benefits and disadvantages reported by Da Luz et al. [26] and Aissani et al. [36], the current metal, A516 Grade 70 carbon steel, predominantly exhibited an α-Fe-pearlite structure, consistent with Feng et al. [29]. They confirmed that a well-applied medium-carbon α-Fe-pearlite mixture achieved high strength, with good agreement in microstructural evolution. While it offers superior advantages, including industry popularity and economic benefits, A516 Grade 70 carbon steel is more susceptible to corrosion in both ambient and high-temperature environments.

4.0 CONCLUSION

This paper demonstrated the benefits of A516 Grade 70 carbon steel, which is widely used across many industries. In this paper, we have thoroughly examined the tensile, bending, hardness, and microstructural properties of A516 Grade 70. The tensile, bending, and hardness test results support existing findings that A516 Grade 70 is well suited for the fabrication industry. Employing this type of carbon steel, a mixture of medium-carbon α-Fe-pearlite, can provide high-strength advantages with good agreement in microstructural evolution. A516 Grade 70 carbon steel exhibits high mechanical performance under stress, with valuable low-cost characteristics that make it the most widely used steel in commercial plants or the oil and gas industry. Overall, A516 Grade 70 carbon steel offers a well-balanced combination of tensile strength, bendability, hardness, and favorable microstructural characteristics, making it an excellent choice for applications requiring high strength and reliable performance. By incorporating these findings, future studies can build on the established data to explore advanced treatments, alloying techniques, or alternative applications. Furthermore, the reliable data presented here can support the development of improved standards and guidelines for using A516 Grade 70 across various industrial contexts.

ACKNOWLEDGMENTS

The authors extend their gratitude to Universiti Kuala Lumpur for the financial support provided under the short-term research grant for the UNIKL/CORI/STR19020 project. They also appreciate the support from Universiti Kuala Lumpur Malaysia France Institute (UNIKL MFI) and the Science and Technology Research Institute for Defense (STRIDE) Kajang for providing the necessary facilities and a conducive environment for conducting this research.

AUTHOR CONTRIBUTIONS

H. Muhamad Hellmy: Conceptualization, Methodology, Investigation, Formal Analysis, Data Curation, Writing – Original Draft Preparation;

C. L. Nur Azida: Validation, Methodology, Supervision, Writing – Review and Editing, Project Administration; M. Z. Norazwani: Investigation, Experimental Work, Data Collection, Data Curation, Formal Analysis, FESEM-EDS Analysis, Writing – Review and Editing.

CONFLICTS OF INTEREST

The manuscript has not been published elsewhere and is not under consideration by other journals. All authors have approved the review, agreed with its submission, and declared no conflict of interest in the manuscript.

REFERENCES

[1] G. Musalaiah, B. V. Suresh, P. Srinivasa Rao and P. Govinda Rao, "Shear strength enhancement in vibratory lap welded joint", *International Journal of Mechanical Engineering and Technology*, vol. 8, no. 1, pp. 160–168, 2017.

[2] P. Sakthivel, V. Manobbala, T. Manikandan, Z. M. A. Salik and G. Rajkamal, "Investigation on mechanical properties of dissimilar metals using MIG welding", *Materials Today: Proceedings*, vol. 37, no. 2, pp. 531–536, 2021.

[3] J. Linares, M. González and C. Herrera, "Ductile fracture behavior of ASTM A516 Gr.70 pressure vessel steel by ASTM and ISO fracture toughness standards", *Metals*, vol. 15, no. 5, 867, 2023.

[4] R. Suraj, "Hardfacing and its effect on wear and corrosion performance of various ferrous welded mild steels", *Materials Today: Proceedings*, vol. 42, pp. 842–850, 2021.

[5] K. Chong, E. E. Mhd Noor, A. Amir and M. F. Baig, "Study on welding characteristics and parameters of gas metal arc welding for A516 Grade 70 steel with ER70S-6 and ER308LSi filler materials", *Materials*, vol. 17, no. 21, 5391, 2024.

[6] N. A. C. Lah, A. Ali, N. Ismail, L. P. Chai and A. A. Mohamed, "The effect of controlled shot peening on fusion welded joints", *Materials & Design*, vol. 31, no. 1, pp. 312–324, 2010.

[7] A. I. Gordienko, L. S. Derevyagina, A. G. Malikov, N. S. Surikova and M. N. Volochaev, "The effect of the initial microstructure of the X70 low-carbon microalloyed steel on the heat affected zone formation and the mechanical properties of laser welded joints", *Materials Science and Engineering: A*, vol. 797, 140075, 2020.

[8] Y. M. Pusparizkita, V. A. Fardilah, C. Aslan, J. Jamari and A. P. Bayuseno, "Understanding of low-carbon steel marine corrosion through simulation in artificial seawater", *AIMS Materials Science*, vol. 10, no. 3, pp. 499–516, 2023.

[9] C. Prieto, C. Barreneche, M. Martínez, L. F. Cabeza and A. I. Fernández,

"Thermomechanical testing under operating conditions of A516Gr70 used for CSP storage tanks", *Solar Energy Materials and Solar Cells*, vol. 174, pp. 509–514, 2018.

[10] A. B. Ibrahim, F. A. Al-Badour, A. Y. Adesina and N. Merah, "Effect of process parameters on microstructural and mechanical properties of friction stir diffusion cladded ASTM A516-70 steel using 5052 Al alloy", *Journal of Manufacturing Processes*, vol. 34, pp. 451–462, 2018.

[11] R. Oyyaravelu, P. Kuppan and N. Arivazhagan, "Metallurgical and mechanical properties of laser welded high strength low alloy steel", *Journal of Advanced Research*, vol. 7, no. 3, pp. 463–472, 2016.

[12] R. Bakhtiari and S. Zangeneh, "Evaluation of hydrogen damage in a fire tube using microstructure/mechanical properties studies", *Engineering Failure Analysis*, vol. 90, pp. 231–244, 2018.

[13] P. J. Prajapati and V. J. Badheka, "Investigation on three different weldments on performance of SA516 Gr70 steel material", *Alexandria Engineering Journal*, vol. 58, no. 2, pp. 637–646, 2019.

[14] H. H. Huang, W. T. Tsai and J. T. Lee, "The influences of microstructure and composition on the electrochemical behavior of A516 steel weldment", *Corrosion Science*, vol. 36, no. 6, pp. 1027–1038, 1994.

[15] F. J. Ruiz-Cabañas, A. Jové, C. Prieto, V. Madina, A. I. Fernández and L. F. Cabeza, "Materials selection of steam-phase change material (PCM) heat exchanger for thermal energy storage systems in direct steam generation facilities", *Solar Energy Materials and Solar Cells*, vol. 159, pp. 526–535, 2017.

[16] F. Badkoobeh, A. Nouri, H. Hassannejad and H. Mostaan, "Microstructure and mechanical properties of resistance spot welded dual-phase steels with various silicon contents", *Materials Science and Engineering: A*, vol. 790, p. 139703, 2020.

[17] Y. Otani and S. Sasaki, "Effects of the addition of silicon to 7075 aluminum alloy on microstructure, mechanical properties, and selective laser melting processability", *Materials Science and Engineering: A*, vol. 777, p. 139079, 2020.

[18] P. Corigliano, V. Crupi, E. Guglielmino and A. M. Sili, "Full-field analysis of AL/FE explosive welded joints for shipbuilding applications", *Marine Structures*, vol. 57, pp. 207–218, 2018.

[19] B. Kim, S. Kim and H. Kim, "Effects of alloying elements (Cr, Mn) on corrosion properties of high-strength steel in 3.5% NaCl solution", *Advances in Materials Science and Engineering*, vol. 1, pp. 1–14, 2018.

[20] A. Taherinia, A. Eslami, M. A. Golozar and F. Fadaeifard, "High-temperature creep analysis of carbon steel A516-Gr70 used in thin-walled pressure vessels under different loads at constant temperature", *Materials Science and Engineering: A*, vol. 857, p. 144054, 2024.

[21] L. Jintang, C. Chunshan, K. Gang, X. Qiaoyu and C. Jinhong, "Influence of silicon on the α-Fe/Γ interface of hot-dip galvanized steels", *Surface and Coatings Technology*, vol. 200, nos. 18–19, pp. 5277–5281, 2006.

[22] S. Noor-E-Khuda, F. Albermani and M. Veidt, "Flexural strength of weathered granites: Influence of freeze and thaw cycles", *Construction*

and Building Materials, vol. 156, pp. 891–901, 2017.

[23] M. Bellavoine, M. Dumont, M. Dehmas, A. Stark, N. Schell, J. Drillet, V. Hebert and P. Maugis, "Ferrite recrystallization and austenite formation during annealing of cold-rolled advanced high-strength steels: In situ synchrotron X-ray diffraction and modeling", *Materials Characterization*, vol. 154, pp. 20–30, 2019.

[24] M. A. Khan, A. Shah, S. H. I. Jaffery, M. Khan and A. R. Khan, "Analysis of surface treatment of ASTM A516 Grade 70 using salt spray method", *IOP Conference Series: Materials Science and Engineering*, vol. 689, no. 1, pp. 1–6, 2019.

[25] K. Sivakumar, M. Saravana, S. Balaguru, R. Sabarish and J. Manikandan, "Mechanical characteristics of gas metal arc welding of ASTM A516 grade 70 steel", *International Journal of Applied Engineering Research*, vol. 10, no. 68, pp. 822–828, 2015.

[26] F. S. Da Luz, W. A. Pinheiro, S. N. Monteiro, V. S. Candido and A. C. R. Da Silva, "Mechanical properties and microstructural characterization of a novel 316L austenitic stainless steel coating on A516 Grade 70 carbon steel weld", *Journal of Materials Research and Technology*, vol. 9, no. 1, pp. 636–640, 2020.

[27] M. Yu, C. Wei, L. Niu and Y. Yu, "Calculation for tensile strength and fracture toughness of granite with three kinds of grain sizes using three-point-bending test", *PLoS ONE*, pp. 1–20, 2018.

[28] J. Saewe, N. Carstensen, P. Kürnsteiner, E. A. Jägle and J. H. Schleifenbaum, "Influence of increased carbon content on the processability of high-speed steel HS6-5-3-8 by laser powder bed fusion", *Additive Manufacturing*, vol. 46, 102125, 2021.

[29] H. Feng, L. Cai, L. Wang, X. Zhang and F. Fang, "Microstructure and strength in ultrastrong cold-drawn medium carbon steel", *Journal of Materials Science & Technology*, vol. 97, pp. 89–100, 2022.

[30] S. K. Alias, B. Abdullah, A. Jaffar, S. A. Latip, S. Kasolang, M. F. Izham and M. A. A. Ghani, "Mechanical properties of paste carburized ASTM A516 steel", *Procedia Engineering*, vol. 68, pp. 525–530, 2013.

[31] C. Sun, P. -X. Fu, X.-P. Ma, H. -H. Liu, N. -Y. Du, Y. -F. Cao, H. -W. Liu and D. -Z. Li, "Effect of matrix carbon content and lath martensite microstructures on the tempered precipitates and impact toughness of a medium-carbon low-alloy steel", *Journal of Materials Research and Technology*, vol. 9, no. 4, pp. 7701–7710, 2020.

[32] O. S. Zaroog, S. A. P. Sughanthy, M. R. Isa and M. N. M. Ansari, "Improving ASTM A516 grade 70 mechanical properties by sandblasting process," *International Journal of Engineering and Technology (UAE)*, vol. 7, no. 4, pp. 216–218, 2018.

[33] F. Zarei, H. Nuranian and K. Shirvani, "Effect of Si addition on the microstructure and oxidation behaviour of formed aluminide coating on HH309 steel by cast-aluminizing," *Surface and Coatings Technology*, vol. 394, 125901, 2020.

[34] C. Chen, H. Xue, H. Peng, L. Yan. L. Zhi and S. Wang, "Inclusions and microstructure of steel weld deposits with nanosize titanium oxide addition", *Journal of Nanomaterials*, vol. 2014, pp. 1-7, 2014.

[35] A. N. Vasileiou, M. C. Smith, J. A. Francis, J. Balakrishnan, Y. L. Wang, G. Obasi, M. G. Burke, E. J. Pickering, D. W. Gandy and N. M. Irvine, "Development of microstructure and residual stress in electron beam welds in low alloy pressure vessel steels", *Materials & Design*, vol. 209, p. 109924, 2021.

[36] L. Aissani, A. Alhussein, A. Belgroune, C. Nouveau, E. Zgheib, R. Barille and A. Montagne, "Effect of carbon content on structural, mechanical and tribological properties of Cr-V-C-N coatings", *Thin Solid Films*, vol. 732, p. 138782, 2021.